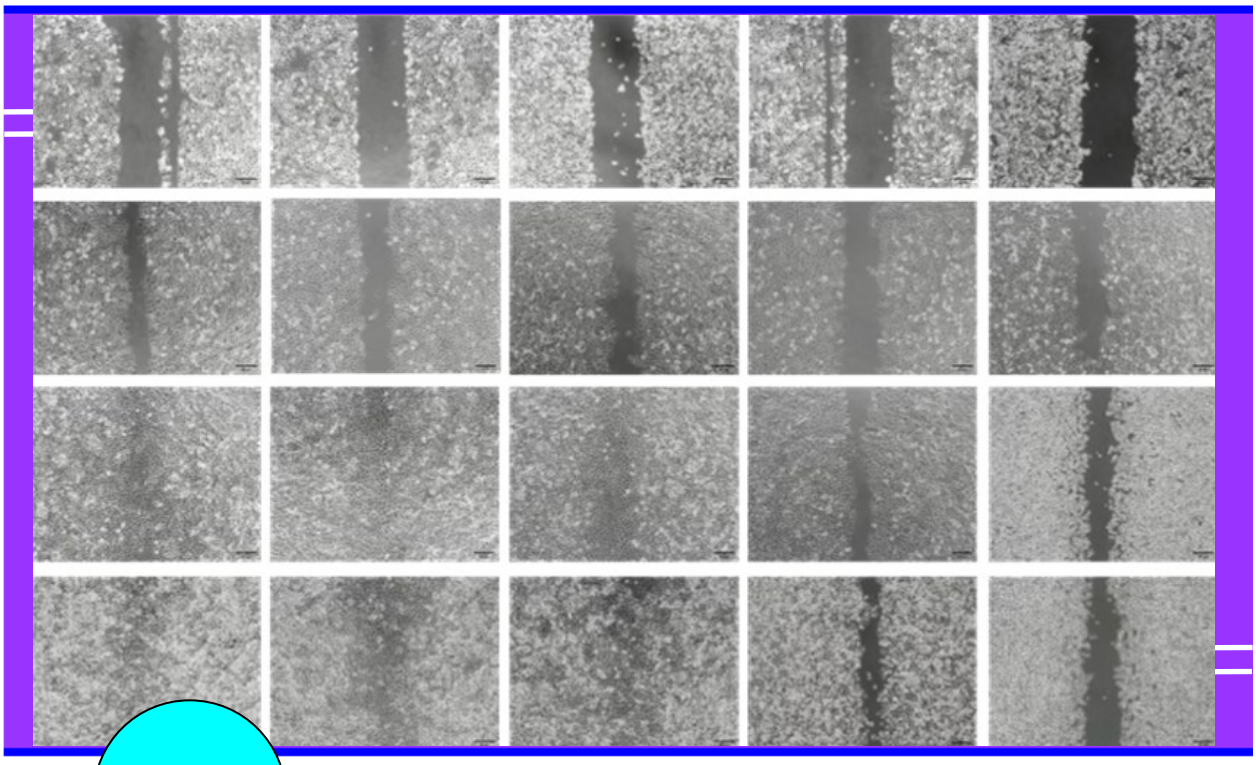

BJP

Bangladesh Journal of Pharmacology

Research Article

Effects of ethanolic leaf extract of *Gynura divaricata* on *NF-κB* pathway in human HeLa cells

A Journal of the Bangladesh Pharmacological Society (BDPS)
Journal homepage: www.bdpsjournal.org; www.banglajol.info
Abstracted/indexed in Academic Search Complete, Agroforestry Abstracts, Asia Journals Online, Bangladesh Journals Online, Biological Abstracts, BIOSIS Previews, CAB Abstracts, Current Abstracts, Directory of Open Access Journals, EMBASE/Excerpta Medica, Global Health, Google Scholar, HINARI (WHO), International Pharmaceutical Abstracts, Open J-gate, Science Citation Index Expanded, SCOPUS and Social Sciences Citation Index
ISSN: 1991-0088

Bangladesh J Pharmacol 2026; 21: 72-83

Effects of ethanolic leaf extract of *Gynura divaricata* on *NF-κB* pathway in human HeLa cells

Kuan-Hung Lin[1], Shao-Wei Huang[2], Shwu-Fen Pan[2], Yi-Hung Li[3], and Chih-Ming Chiang[2]

[1]Department of Horticulture and Biotechnology, Chinese Culture University, Taipei 11114, Taiwan; [2]Department of Biotechnology, Ming Chuan University, Taoyuan 333348, Taiwan; [3]Department of Biotechnology and Animal Science, National Ilan University, Yilan 260007, Taiwan.

Article Info

Received: 12 June 2026
Accepted: 26 June 2026
Available Online: 26 June 2026
DOI: 10.3329/bjp.v21i2.90797

Cite this article:
Lin KH, Huang SW, Pan SF, Li YH, Chiang CM. Effects of ethanolic leaf extract of *Gynura divaricata* on *NF-κB* pathway in human HeLa cells . Bangladesh J Pharmacol. 2026; 21: 72-83.

Abstract

This study aims to evaluate the anti-cancer activity of the ethanolic leaf extract of *Gynura divaricata* in human cervical cancer HeLa cells. Cells were treated with various concentrations of extract, and cell viability was assessed to determine the half-maximal inhibitory concentration (IC_{50}). The extract significantly reduced HeLa cell viability in a concentration-dependent manner, demonstrating marked cytotoxic activity. Treatment with 2x IC_{50} extract markedly suppressed cellular metabolic activity and significantly downregulated the expression of NF-κB-related genes compared with control and DMSO-treated cells. The extract also reduced the transcription of inflammatory and apoptosis-associated factors, including TNF-α, Bcl-2, Bax, COX-2, IKKα, IκBα, IL-8, IL-6, and IL-1β. These findings indicate that *G. divaricata* inhibits HeLa cell growth by suppressing NF-κB-mediated signaling and inflammatory responses, suggesting its potential as a natural therapeutic agent against cervical cancer.

Introduction

The use of natural antioxidants as pharmaceutical products and functional foods has gained considerable attention, and the antioxidant ability and biological properties of various natural extracts are correlated with the plant sources from which they are derived (Lin et al., 2019). One of these plants, the Taiwanese native species *Gynura divaricata* Formosana, is an edible flower -ing perennial plant in the family Asteraceae. It is mostly planted in southern Taiwan. It a valuable and economically significant herbal plant with notable economic potential. Young leaves of *G. divaricata* are commonly consumed in Taiwan as tea or salad garnish, as a natural health food, and historically used in traditional Chinese medicine to treat hepatitis and liver cancer (Kantawong et al., 2021). Furthermore, the components of *G. divaricata* have been studied for their various bioactivities, and are widely treated as a folk medicinal tonic in Asia (Chao et al., 2014; Nadechanok et al., 2015; Xu et al., 2017; Ma et al., 2018). For example, *G. divaricata* extracts have been used to treat diabetes, hypertension, hyperlipidemia, hyperglycemia, and many other ailments for their anti-cancer effects (Chou et al., 2012; Chen et al., 2014; He et al., 2014; Jin et al., 2018; Yen et al., 2018; Dong et al., 2019; Hong et al., 2020; Ye et al., 2022; Xu et al., 2024; Rifai et al., 2024; Shen et al., 2025).

Transcription factor nuclear factor (NF)-kB plays a key

role in inflammatory responses and cancer development by regulating genes involved in angiogenesis and tumorigenesis during molecular signaling in the NF-kB pathway. Elevated NF-κB activity contributes to increased levels of pro-inflammatory cytokines; therefore, the NF-κB signaling pathway is considered a potential therapeutic target for cancer therapy (Feng et al., 2023). The expression levels of NF-kB, cyclooxygenase (COX)-2, and multigenes have shown significant associations with poor survival and increased tumor aggressiveness in human cervical cancer samples (Pasha et al., 2024). Black soybean seed coat extracts inhibit tumor necrosis factor (TNF)-*a*-induced COX-2 levels through an NF-κB -dependent pathway, and have anti-inflammatory effects on an immortalized epidermal keratinocyte cell line (Kim et al., 2012). It has anti-inflammatory and anti-atherogenic effects on TNF-*a*-induced cell adhesion in human aortic endothelial cells (HAEC) by regulating NF-κB (Chao et al., 2013a). In addition, TNF-*α*-induced HAEC adhesion is significantly suppressed by mulberry leaf extracts, resulting in reduced expression of NF-*κ*B (Chao et al., 2013b). Moreover, extract of sweet potato leaves shows anti-inflammatory effects via reducing mitogen-activated protein kinase (MAPK) and NFκB expressions, inhibiting TNF-α-induced monocyte -endothelial cell adhesion, and attenuating interleukin-8 (IL-8) and vascular cell adhesion molecule-1 (VCAM-1) expressions (Lee et al., 2015). The consumption of purple sweet potato leaves modulates various immune functions, including the secretion of cytokines IL-2 and IL-4 of natural killer cells and induces an increase in proliferation responsiveness in peripheral blood mononuclear cells (Chen et al., 2005). Moreover, purple leaf extracts also depress neuroinflammatory responses in lipopolysaccharide-activated BV-2 microglia cells by inhibiting the production of inflammatory mediators such as inducible COX-2 and TNF-α (Kang et al., 2014). *G. divaricata* water extract inhibits NF-*κ*B activation and reduces insulin pathway deficiencies, such as IRS1, AKT, and GLUT1 (Li et al., 2018). In addition, aqueous extracts reduce the levels of IL-6 and TNF-α and increase the levels of VEGFA mRNA and protein expression in rats (Sun et al., 2023). It has hypoglycemic effects *in vivo* by regulating the genes at PI3K/AKT and fatty acid metabolism signaling pathway, and the Bcl-2/Bax expression ratio in the liver of rats is significantly upregulated after *G. divaricata* intervention (Xu et al., 2020).

However, the cytotoxic effects of *G. divaricata* leaf extract on human cervical cancer HeLa cells and the underlying molecular mechanisms remain largely unknown. NF-κB signaling plays an important role in cancer progression and oxidative stress regulation. Therefore, this study investigated the effects of ethanolic *G. divaricata* leaf extract on HeLa cell viability, antioxidant activity, and NF-κB-related gene expression. Antioxidant capacity was evaluated using 2,2-diphenyl-1-picrylhydrazyl (DPPH), ferric reducing antioxidant power (FRAP), malondialdehyde (MDA), hydrogen peroxide (H_2O_2), and antioxidant enzyme assays. The findings provide insights into the antioxidant and anticancer potential of *G. divaricata* and its possible application as a plant-derived complementary therapeutic agent.

Materials and Methods

Plant material and culture practice

Young *G. divaricata* plantlets were originally collected from a local farmer's field in the Peito mountain area, Taipei, Taiwan (25°07′12″ N, 121°30′36″ E). The subspecies was authenticated and identified according to the List of Plants of Formosa at the National Taiwan University herbarium (https://tai2.ntu.edu.tw/species/). The surfaces of stem explants (15 cm long) with 3 -paired leaves were propagated in 5-inch plastic pots, one plant per pot, filled with commercial potting soil with a substrate mixture of peat moss, perlite, and vermiculite (3:1:1 v/v/v, Known-You Co., Taiwan). They were then placed in a growth chamber for two months. The average temperature in the growth chamber was 25°C, with day lengths of 16 hours in 1,600 lux/m^2 and 80% relative humidity. Plants were watered twice daily, and a compound fertilizer solution (N-P_2O_5-K_2O, 20-20-20) was applied once a week. Uniformly sized plants were randomly chosen for further experiments.

Extraction of leaves

Fresh leaves of *G. divaricata* were extracted by maceration using 95% ethanol as the solvent at a ratio of 1:10 (w/v) for 2 hours (Kalsoom et al., 2024) with a shaker at 100 rpm under in a 50 L glass bottle at room temperature, followed by centrifuging (Kubota 3740, Japan) at 12,000 rpm for 10 min at 4°C (Hou et al., 2005). Supernatants were filtered and freeze-dried using a vacuum evaporator (FDM-2000, Eyela, Japan) to remove the solvent until a fat with viscous wax was obtained. The ethanol-free extract was then stored at -20°C until used.

Cell culture treatment and cell viability test

Human cervical epithelioid carcinoma HeLa cells (#60005) were purchased from the Bioresource Collection and Research Center of the Institute of Food Industry, Hsinchu City, Taiwan. The cells were cultured and maintained in Dulbecco's modified Eagle's medium (DMEM) (D5648, Sigma-Aldrich, USA) supplemented with 10% fetal bovine serum (FBS) and 1.5% penicillin-streptomycin antibiotic solutions in 10 cm Petri dishes at 37°C with a 5% CO_2 atmosphere as previously described (Ma et al., 2018) within an incubator (SCA150-Astec, Japan). After the cultured cells reached 80% confluency, they were treated with trypsin, and the

cleaved cells were counted under an inverted microscope (AMEX1000, Life Technologies, USA) using a cell counting plate. Plates were divided according to the number of cells and seeded into new culture plates at a density of 10^5 cells/ mL for sub-culturing.

The 3-(4,5-dimethylthiazol-2-yl)-2,5-diphenyltetrazolium bromide (MTT) assay, by the reduction of MTT in active mitochondrion to purple formazan, was used to determine the effects of potential agents or compounds on the proliferation of cells to assess cell viability (Kumar et al., 2018). Briefly, 5,000 cells in a well were plated in a 96-well plate and kept at 37°C with 5% CO_2 for a day. After the medium was removed, HeLa cells were exposed to different concentrations of *G. divaricata* extract for another 24 hours. HeLa cells that cultured in normal complete DMEM (not treated with extract) served as the control. When incubation was completed, media were discarded, and cells were post-treated by exposure to 0.5 mg/mL MTT (Invitrogen Inc., USA) and further incubated for 4 hours at 37°C. After incubation, the media were discarded, and cells were then washed with phosphate-buffered saline (PBS), followed by dissolving in 100 µL of dimethyl sulfoxide (DMSO) in the well and then incubated for 1 hour. Absorbance was subsequently determined using an enzyme-linked immunosorbent assay (ELISA) micro-plate reader (Spectra Max 190, USA) at a wavelength of 570 nm. Absorbance readings were converted into percentages of cells viable by comparing the treated group of each concentration with untreated controls. The IC_{50} value was determined by performing linear regression between the concentration (x) and % cell viability (y). Cell viability % was measured as

$$[(\text{control} - \text{blank}) / (\text{sample} - \text{blank})] \times 100\%$$

where control, sample, and blank were the extract-untreated group, extract -treated group, and DMSO-only group, respectively

The IC_{50} value represents the concentration that inhibited 50% of cell proliferation, and the experimental data for this research was obtained from three independent replication experiments. After percent cell viability was observed, their values were used for making the standard curve with a linear equation.

Cell migration assay

Cell migration is an important factor to consider when investigating the metastatic potential of cancer cells, and cell adhesion to extracellular matrices is considered to be a pivotal step in the invasive process of metastatic cells. The abovementioned DMSO (1 µL/mL), and extract dissolved in DMSO to concentrations of 500, 1000, and 2000 ng/mL as 0.5x IC_{50}, 1x IC_{50}, and 2x IC_{50} concentrations, respectively, were cultured for 24 hours at 37°C.

Crude protein was extracted based on the protocol from Yoon and Moon (2021). Centrifugation was performed to remove the medium, and cells were harvested and washed with cold PBS. Samples were incubated with 1 mL RIPA lysis buffer (containing 20 mM Tris, 5 mM EDTA, 10 mM Na_3PO4, 100 mM NaF, 1% Nonidet P-40, and 1 mM PMSF at pH 7.4, RB4475, ProTech, Taiwan) and 10 µL of protease inhibitor (P8340, Sigma-Aldrich, USA). Thereafter, the cell layer was scratched with a cell scraper (BD Falcon, Corning, USA) to remove cells, placed into a 1.5 mL tube, and vortexed for 1 min. The crude protein was centrifuged at 13,000 rpm and 4°C for 1 min, and the supernatant then collected. Total soluble protein was quantified with a Bradford Protein Assay Kit (BioRad, USA). The amount of crude protein concentration was determined at an optical density of 595 nm using an ELISA reader. Commercial bovine serum albumin (BSA-A9418, Sigma) was used as a standard of linear regression equation.

HeLa cells were left untreated or treated with 0x, 0.5x, 1x, and 2x IC_{50} concentrations of extract for 24 hours at 37°C, seeded in a 24-well plate, and grown overnight to confluency in DEME-containing medium for 48 hours. After removing the medium, the confluent cell layer was scratched with a p200 Eppendorf pipette tip (Justus et al., 2014). Scraped cells were then washed away with PBS, and extract was added at 0x, 0.5x, 1x, and 2x IC_{50} concentrations (with a final concentration of 4 µL/mL in the micro-plate wells). The plates were incubated for 0, 24, 48, and 72 hours, followed by counting the cells using ImageJ (1.05d, 64-bit Java 8, NIH, USA). The closure of the scratch wound area was photographed from three different images captured at a magnification of 10-fold using an inverted microscope. Triplicate controls and triplicate test samples were prepared for each time point in duration of 72 hours.

Determination of H_2O_2 content and lipid peroxidation

H_2O_2 content was determined according to Rahman et al. (2023). Briefly, 0.1 mL extract was homogenized in 0.1 mL of sodium phosphate buffer (10 mM, pH 7.0) containing 1 mM hydroxylamine and centrifuged at 8,000 rpm for 25 min at 4°C. One mL of the supernatant was then mixed with 0.5 mL of titanium chloride ($TiCl_4$, 0.1% v/v) dissolved in 20% (v/v) sulfuric acid (H_2SO_4), followed by centrifuging again at 3,300 rpm for 15 min at room temperature. The supernatant was transferred to a 96-well microplate (SpectraMax-190) and measured at 390 nm (A_{390}). Distilled-deionized water was used as the blank, and H_2O_2 concentration (µmol/mg protein) was calculated based on the standard calibration curve with 5, 10, 15, 20, 25 µmol H_2O_2.

Lipid peroxidation was evaluated by quantifying MDA, a commonly used indicator, based on Kosugi and Kikugawa (1985). In brief, 0.1 mL extract was homogenized

in 1.5 mL 5% (w/v) trichloroacetic acid (TCA) and centrifuged at 10,000 rpm for 5 min at 20°C. Supernatant (0.2 mL) was thoroughly mixed with 0.8 mL of 0.5% (W/V) thiobarbituric acid prepared in 20% (W/V) TCA, and incubated in a circulating dry bath (Sahara Rocker, Taiwan) at 95°C for 30 min. After cooling, samples were centrifuged again at 6,000 rpm for 10 min, and the supernatant then measured at 532 nm (A_{532}) using a spectrophotometer. TCA (5% w/v) was used as the blank. MDA concentration (µmol/mg) was calculated using the following equation:

A_{532} / 1.56 × 10^5 (L mol^{-1} cm^{-1}) × 1 (dilution factor) / protein (mg)

Determination of antioxidant activity

To analyze the activity of ascorbate peroxidase (EC 1.11.1.11) and catalase (EC 1.11.1.6), 100 mg of leaf powder was extracted with 100 mM sodium phosphate buffer (pH 6.8) containing 1 mM phenylmethylsulfonyl fluoride (Sigma). Ascorbate peroxidase and catalase activity was measured according to the protocols of Nakano and Asada (1981). Absorbance was measured at 290 nm in a UV–visible spectrophotometer, and one unit was defined as micromoles of ascorbate oxidized per minute (extinction coefficient 2.8 mM cm^{-1}). Further -more, one unit of catalase activity was defined as the amount of enzyme catalyzing the decomposition of 1 nmol H_2O_2 per minute, with an extinction coefficient of 36 mM cm^{-1}. Glutathione reductase (EC 1.6.4.2) activity was measured by the GSH-dependent oxidation of NADPH according to Foyer et al. (1997). Superoxide dismutase (EC 1.15.1.1) activity was assayed by using the protocol of Dhindsa et al. (1981), and absorbance was recorded at 560 nm in a spectrophotometer.

Measurements of DPPH radical-scavenging ability and reducing power capacity

The antioxidant activity of extract was determined by DPPH scavenging capacity and reducing power ability. The assessment of scavenging activity against free DPPH radicals followed the protocols outlined by Wan et al. (2011). Briefly, 100 µL of the abovementioned control, DMSO, 0.5x IC_{50}, 1x IC_{50}, and 2x IC_{50} in culture medium DMEM were mixed with 100 µL 0.2 mM of DPPH (Sigma) and incubated in the dark at room temperature for 30 min. After centrifuging at 13,000 rpm for 1 min, the supernatant was placed into a 96-well ELISA microplate reader. The mixture was kept in the dark for 20 min, during which its color changed from purple (DPPH radical) to yellow (DPPH-H) following reduction. This change in color, quantified by a decrease in absorbance at wavelength 517 nm, indicates DPPH scavenging activity. A lower absorbance denotes higher DPPH-scavenging activity, and radical-scavenging activity is directly proportional to the concentrations of the extracts. Optical densities were calculated for % inhibition using the following equation:

DPPH radical scavenging activity (%) = [1- (sample) / (blank)] x 100%

Blanks were prepared in the same manner, using ethanol in place of extract samples. Triplicate controls and samples were prepared for each concentration presented in the form of mean ± SD in the DPPH test.

G. divaricata extract reducing power activity was determined by the ferric reducing antioxidant power (FRAP) assay of Oyaizu et al. (1998). Briefly, 100 µL of control and extract samples were mixed with 100 µL of 0.2 M sodium phosphate buffer (pH 6.6) and 100 µL of 1% potassium hexacyanoferrate. The mixture was incubated at 50 °C for 20 min. After cooling on ice, 100 µL of 10% TCA was added to the mixture, vibrated for 5 min, and then centrifuged at 10,000 rpm for 10 min. The supernatant was then mixed with 100 µL 1% ferric chloride. After 10 min, absorbance at 700 nm using an ELISA plate reader was measured against a blank. FRAP (mmol vitamin C/µg protein) was assessed using the following equation:

FRAP = OD_{700}/ 1.77 × 10^4 (L/mol/cm) × 0.5 (total volume, mL) × 0.1 (sample volume, mL) ×10 (dilution fold) × 0.1 (sample extract, g / mL)

A blank was prepared using water without sample, and vitamin C used as a standard. The existence of reductants in the solution causes the reduction of the ferric to the ferrous form, and an increase in absorbance of the sample with various concentrations indicates a high reducing power capacity of the samples.

Western blotting

The effect of extract on NF-κB was determined by immune-blotting according to Xu et al. (2020). Briefly, total proteins were extracted from the abovementioned controls, DMSO, 0.5x IC_{50}, 1x IC_{50}, and 2x IC_{50} of extract, by incubating with RIPA lysis buffer (pH 7.4) for 30 min on ice, with agitation every 10 min. After centrifugation for 15 min at 10,000 rpm and 4°C, the supernatant was collected and the protein concentration determined based on the Bradford protein assay (1976). Equal amounts of crude protein (20 µg/lane) were resolved in 10% sodium dodecyl sulfate-poly-acrylamide gel electrophoresis (SDS-PAGE) gels (Mini -Protein Tetra, Bio-Rad, USA), separated at 20 mA for 2 hours, and transferred onto polyvinylidene difluoride membrane (Immobilon®-P, Millipore, USA) at 200 V and 4°C for 2 hours. After blocking with 5% skimmed milk at 4°C for 2 hours, membranes were incubated overnight at 4°C with primary antibodies against glyceraldehyde 3-phosphate dehydrogenase (GAPDH) XP® rabbit mAb (5174S, Cell Signaling Technology, USA) and anti-NF-κB p65 (ab16502, Abcam, UK) at 1:1000 dilution. Subsequently, the blot was then incubated with goat anti-rabbit IgG H&L horseradish

peroxidase conjugated secondary antibody (ab205718, Abcam, UK) at 1:5000 dilution for 2 hours. Membranes were visualized and detected with a gel documentation system after incubating with chemiluminescent substrate solution for 10 sec (LumiFlash Mltima, Taiwan). Signal intensities were quantified using ImageJ software.

RNA isolation and gene expression analysis

Total RNA was extracted from control and extract -treated HeLa cells using the NucleoZOL extraction kit (Macherey-Nagel, Germany), and treated with DNase I to remove genomic DNA according to the instruction manual. RNA quality and the quality of each sample were determined by agarose electrophoresis and NanoDrop 2000 (Thermo Fisher Scientific, USA), respec -tively. Moreover, mRNAs were purified from 3 µg of total RNA using a MMLV Reverse Transcription Kit (Protech-Bio, Taiwan), followed by RNA converted to complementary (c)DNA under reaction buffers with 0.5 µL (75 ng) cDNA product, 1 µL 10 µM forward and reverse primers (Table I), 4 µL dNTP (2.5 mM), 5 µL Taq DNA polymerase, and 5 µL 10x Taq buffer (Yoon et al., 2021). PCR was carried out in an Eppendorf Mastercycler Gradient Thermal Cycler (Germany) at the following thermal program: initial denaturation at 94°C for 10 min, followed by 30 cycles at 94°C for 30 sec, 57°C for 30 sec, and 72°C for 1 min, with a final extension at 72°C for 10 min. The products were electrophoretically separated on 1.5% agarose gels, predicted size of each gene (Table I) was verified with a 100bp DNA ladder marker (PT-M1-100T, ProTech, Taiwan), and sequences checked.

Table I

Paired primers for RT-qPCR used

Gene		Oligonucleotide sequence	Size (bp)
GAPDH	F	5′-TGTAGGCTCATTTGCAGGGG-3′	
	R	5′-TCCCATTCCCCAGCTCTCAT-3′	317
Bcl-2	F	5′-AAAGCCAGCTTCCCCAATGA-3′	
	R	5′-CCCAACTGCAGGATGCCTTT-3′	596
Bax	F	5′-AACCCTCCTTCAGGGAGTCA-3′	
	R	5′-CTGCAGGGGGTTGATACCAC-3′	423
IL-8	F	5′-GGAAAGTTCCAGGTGTTAGGA-3′	
	R	5′-CACCCAGTTTTCCTTGGGGT-3′	256
TNF-a	F	5′-GAGACAGATGTGGGGTGTGAG-3′	
	R	5′-TCCTAGCCCTCCAAGTTCCA-3′	642
IL-1β	F	5′-GACTTCCCCATGACGGCTAC-3′	
	R	5′-AACCTCTTCGAGGCACAAGG-3′	507
Iκβa	F	5′-TGGCAAATAGCAGAGGCTCC-3′	
	R	5′-TGGGGTTTTTCCCTCTCTTCC-3′	345
COX-2	F	5′-AATGGCTGAGTATGGCACCC-3′	
	R	5′-GCTGTCCTTTAATTGCAGCAAATCC-3′	783
IL-6	F	5′-GCTTCCCTCAGGATGCTTGT-3′	
	R	5′-ATTAACTGGGGTGCCTGCTC-3′	405
NF-κB	F	5′-ATGTGGAGATCATTGAGCAGC-3′	
	R	5′-CCTGGTCCTGTGTAGCCATT-3′	151
IKKa	F	5′-GGCTTCGGGAACGTCTGTC-3′	
	R	5′-TTTGGTACTTAGCTCTAGGCGA-3′	87

F, Forward; R, Reverse. All genes were searched from NCBI (http://www ncbi.nlm.nih.gov/) with *Homo sapiens* (human), and shown as: *GAPDH* (NC_000012.12), *Bcl-2* (NC_000018.10), *Bax* (NC_000019.10), *IL -8* (NC_000004.12), *TNF-a* (NC_000006.12), *IL-1β* (NC_000002.12), *IκBa* (NC_000014.9), *COX-2* (NC_000001.11), *IL-6* (NC_000007.14), *NF-κB*

The relative changes in NF-κB pathway related gene expressions in response to various extract treatments were monitored by real-time (RT) quantitative (q)PCR and quantification of RNA levels. RT-qPCR reactions were assayed with 1 µL of cDNA product, 10 μL of 2X SyGreen mix (BIO Lo-ROX Biosystem Ltc., UK), and 0.8 μL of forward and reverse primers (the final concentration of each the primer was 10 μM) in ddH_2O to a total volume of 20 μL. The RT-qPCR was performed on the ABI 7500 Real-time system (ABI, USA), and the PCR program was set as denature at 95°C for 5 sec, annealing at 60°C for 30 sec, and extension at 72°C performed for 45 cycles. The sequences of paired primers used in this study are presented in Table I. GAPDH was used as a reference gene for normalization, and differential gene expression calculated as follows (Livak and Schmittgen, 2001):

$$2^{-\Delta\Delta Ct} = (Ct_{\text{target gene}} - Ct_{\text{GAPDH}})_{\text{treatment}} - (Ct_{\text{target gene}} - Ct_{\text{GAPD}})_{\text{control}}$$

The control was the cells cultured in complete DMEM, while the treatments were cells cultured in DMSO containing 500, 1,000, and 2,000 ng/mL of extract at 0.5 IC_{50}, 1 IC_{50}, and 2 IC_{50} concentrations. Triplicate control samples and triplicate test samples were prepared and presented as mean ± SD. The independent Student's *t*-test was used to determine differences between control and test groups, and statistical significance was considered when $p<0.05$.

Statistical analysis

All experiments in this study are tabulated as the mean value with the standard deviation (SD) of at least three independent replications, as stated in each figure legend. Student's *t*-test was performed using SAS statistical analysis software Version 9.4 (SAS Institute Inc, USA) to evaluate the statistical comparison of the mean values between two groups. A p-value of less than 0.05 was considered statistically significant.

Results

Effects on the viability of HeLa cells

After measuring absorbance using an ELISA reader, the untreated controls showed the highest cell viability at 100%, and extract significantly reduced HeLa cell viability in a concentration-dependent manner (Figure 1A). In the group treated with 250 ng of extract, the

HeLa cell viability level was reduced to 88.7%, and subsequent concentrations showed a decreasing trend, indicating that extract exerted different cytotoxicity effects on the proliferation of HeLa cells. Extract from 500 to 2,750 ng/mL significantly inhibited the viability of HeLa cells, showing that higher concentrations of extract treatments resulted in progressively lower HeLa cell viability values with higher inhibition rates (%) of repressed cell proliferation. In particular, treatment with 2,000 ng/mL of extract tremendously reduced the viability of HeLa cells (17.9%) compared with the control group (100%). The IC_{50} value was found at 1,000 ng/mL. The Hela cell inhibition rates ranged from 250 to 2,750 ng/mL of extract treatment, the linear curve of regression was y = 0.00484x – 0.3557, with R^2 = 0.9375 (Figure 1B). The inhibitory ability of extract on HeLa cells at a concentration of 1,500 ng/mL entered a plateau which was much stronger than that of other concentrations with 80% of cell inhibition.

Potential effect of extract *on metastasis*

The inhibition of HeLa cell migration was examined using a wound healing assay. The morphologies of HeLa cells were different between controls and extract-treated samples for 0 ~ 72 hours, and all HeLa cells exposed for 24, 48, and 72 hours (20.7 ± 0.7%, 0.8 ± 0.1%, and 0.02 ± 0.01%, respectively) compared to 0 hour at 100% relative wound closure (Figure 2B). After exposure of HeLa cells to DMSO (without extract-treated group) for 24, 48, and 72 hours, significant reduction in adhesion was observed in all cells at 22.9 ± 1.3%, 1.1 ± 0.1%, and 0.01 ± 0.002%, respectively, compared to 0 hour at 100%. The extract at 0.5x IC_{50} (500 ng/mL) significantly reduced the relative wound closure for 24-, 48-, and 72-hours periods at 34.8 ± 1.2%, 10.0 ± 1.7%, and 2.1 ± 0.1%, respectively, compared to 0-hour culture period. After 24, 48, and 72 hours of incubation, 1x IC_{50} extract (1,000 ng/mL)-treated cells showed significantly decreased levels of adhesion (57.2 ± 2.9%, 21.8 ± 1.0%, and 28.9 ± 1.4%) compared to 0 hour of incubation. HeLa cells treated with 2x IC_{50} extract (2,000 ng/mL) for 24, 48, and 72 hours showed less wound healing (56.4 ± 2.9%, 70.7 ± 2.5%, and 73.6 ± 3.4%) than that of the 0 hour group.

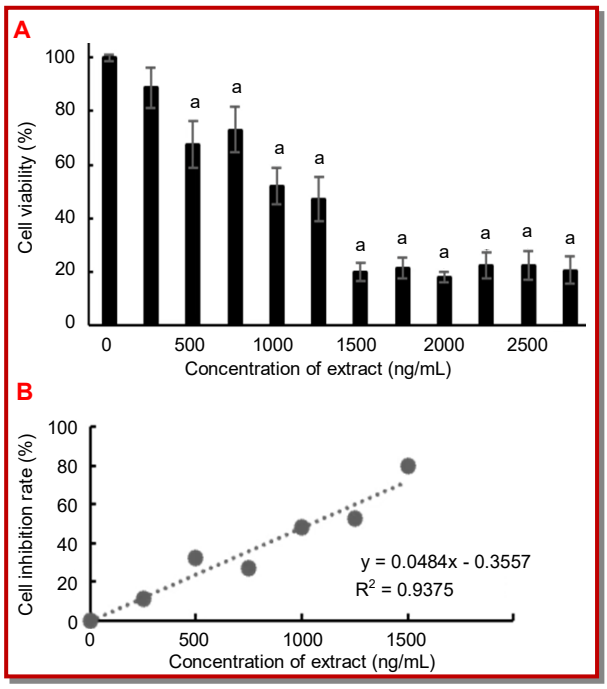

Figure 1: Effect of different concentrations (250 ~ 2,750 ng/mL) of extract treatments on human HeLa cell viability (A) and cell inhibition rate (B) at 48 hours, evaluated by MTT assay. Data are mean ± SD; n=4. $p<0.05$ was considered as statistically significant (superscript "a") compared between control and each concentration of extract treatment using Student's *t*-test

Contents of H_2O_2, MDA, antioxidant activity, and ability of DPPH-scavenging and FRAP

Table II illustrates *G. divaricata* extract significantly alter-ed oxidative stress markers in HeLa cells in a concentration- and time-dependent manner. H_2O_2 levels increased in the 0.5x IC_{50} and 1x IC_{50} treatments after 0.5 hour, whereas prolonged exposure resulted in higher H_2O_2 accumulation in the 1x IC_{50} and 2x IC_{50} groups. MDA contents generally decreased after 24 hours of incubation, with the lowest level observed in the 0.5x IC_{50} treatment, indicating reduced lipid peroxidation.

Among antioxidant enzymes, ascorbate peroxidase activity was not significantly affected by the extract treatment. In contrast, catalase and glutathione reductase activities were reduced at higher extract concentrations, whereas superoxide dismutase activity increased significantly and showed a dose-dependent response. The highest superoxide dismutase activity was detected in the 2x IC_{50} treatment after 24 hours of exposure.

The antioxidant potential of extract was further supported by DPPH and FRAP assays. The extract-treated cells exhibited enhanced radical-scavenging activity, particularly in the 2x IC_{50} treatment, demonstrating that the extract effectively modulated cellular redox status and antioxidant defense mechanisms in HeLa cells.

Western blot of NF-κB from extract

To further elucidate NF-κB mechanisms in extract, the relative amounts (%) of NF-κB accumulation in extract were analyzed by western blot (Figure 3). NF-κB proteins responded differently in the various concentrations of extract-treated HeLa cells, and a clear NF-κB band (60 kDa) appeared in all concentrations (DMSO, 0.5x IC_{50}, 1x IC_{50}, and 2x IC_{50}) and controls. Extract at all concentrations (0.5x, 1x, and 2x IC_{50}) was significantly lower than in controls. As extract E concentration increased, the NF-κB expression level decreased

from controls at 100%, dropping to 20.0% for 2-IC_{50} extract.

Effects of extract on NF-κB-related gene expressions in the NF-κB signaling pathway

Different *NF-κB* related genes involved with extract show differential gene expressions. Human HeLa cells treated with 0.5x, 1x, and 2x IC_{50} of extract showed significant down-regulation of Bcl-2, Bax, IL-8, IKKα, NF-κB, and IL-1β genes (Figure 4A, B, E, G, H, and K, respectively) compared to controls. However, RNA expression of the Bcl-2/Bax gene ratio (Figure 4C) was significantly lower in human HeLa cells treated with 0.5 -IC_{50} of extract than in controls. Significant down-regulations of IL-6, COX-2, and TNF-α genes (Figure 4D, F, and J, respectively) were found in human HeLa cells treated with 1- and 2-IC_{50} of extract compared to controls. Figure 4I shows that RNA abundance of the

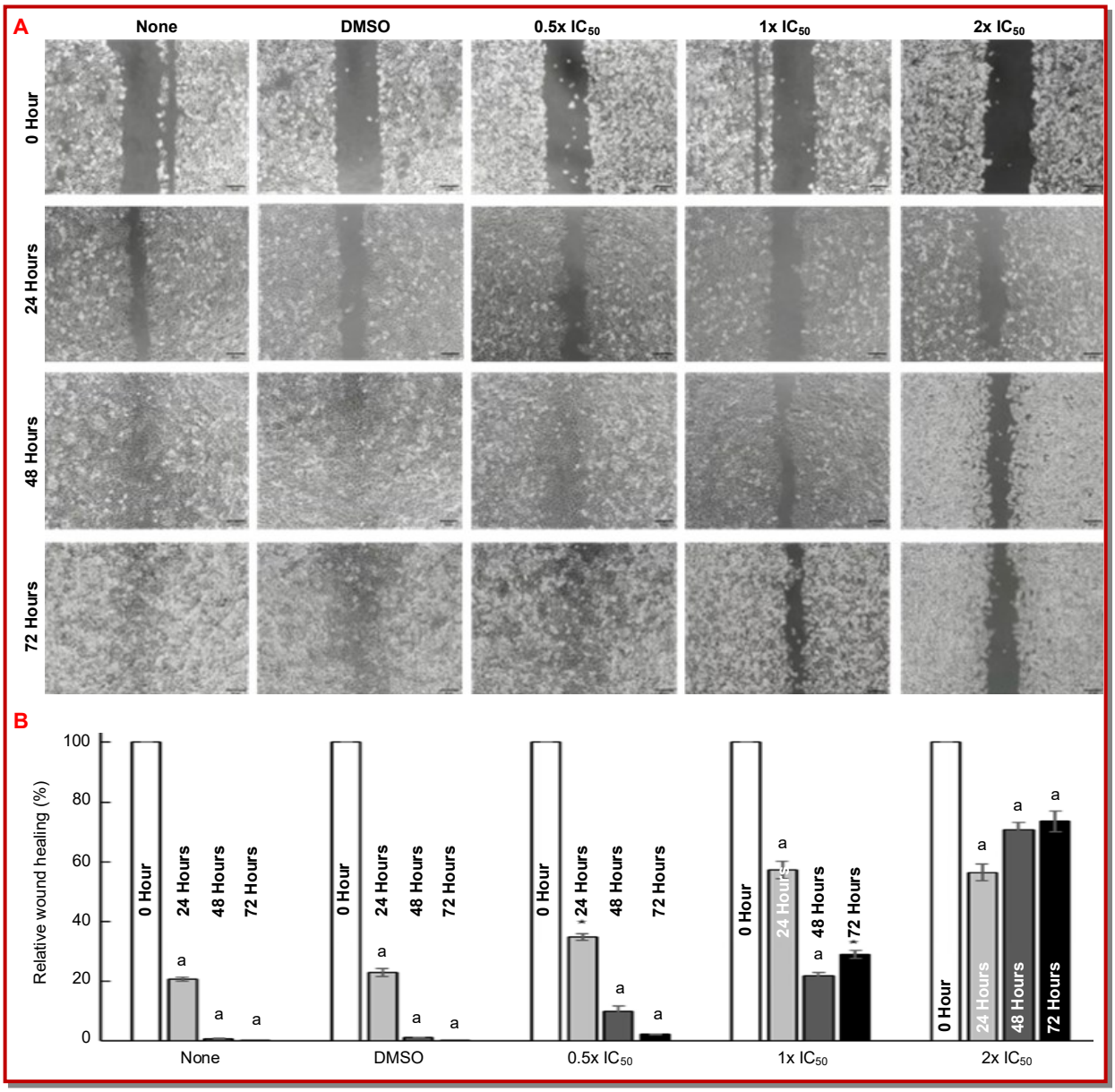

Figure 2: Cell migration assay. Cultured HeLa cells were scratched with a pipette tip, followed by culturing in complete DMEM supplemented with extract at concentrations of 0.5x, 1x, and 2x IC_{50} (calculated as 500, 1,000, and 2,000 ng/mL of extract) and incubated for 72 hours. Controls were cells cultured in complete DMEM, while DMSO was a maintenance medium of extract - untreated cells. Data were collected on incubation day (0 hour) and after 72 hours of incubation, and photographed at 100x magnification. The scale bar at the right corner indicates 20 µm (A) . The closure of the scratch relative wound area (%) from cell morphology photographs was quantified using ImageJ (B). Among each extract concentration treatment, period durations of 24, 48, and 72 hours were compared to 0 (100% as control) using Student's t-test. Triplicate control and triplicate test samples were prepared for each time point, and superscript "a" indicate significance levels of p≤0.05. Vertical bars indicate standard deviations

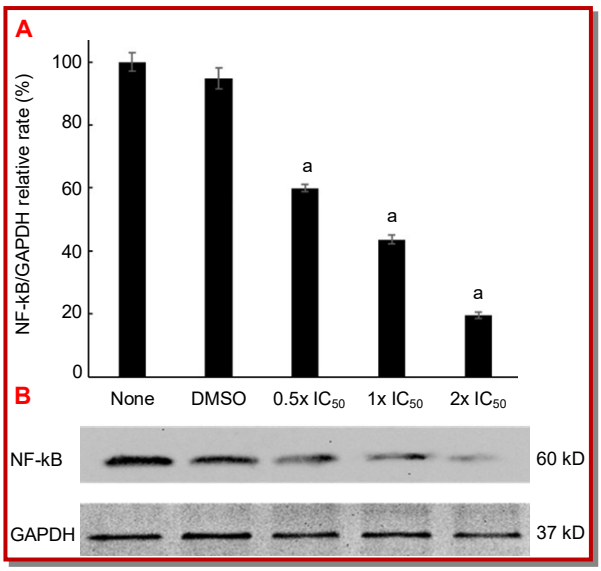

Figure 3: Western blot analysis of HeLa cells cultured in control, DMSO (complete DMEM), and DMSO containing 500, 1,000, and 2,000 ng/mL of extract as 0.5x IC_{50}, 1x IC_{50}, and 2x IC_{50} concentrations, respectively, probed by NF-κB and GAPDH as antibodies. Forty micrograms of total protein were used for each sample during SDS-PAGE separation, and the molecular weights of NF-κB and GAPDH (used as an internal control) are 60 and 37 kDa, respectively, as indicated by two arrowheads. A representative image of three similar results is shown. Bands with NF-κB/GAPDH relative rate (%) were visualized and detected with a chemiluminescent substrate, and intensities are quantified using ImageJ software, followed by representation on the bar graphs. [a]p<0.05 compared to the control is expressed as 100%

IκBα gene was significantly up-regulated in DMSO and 0.5-IC_{50} of extract-treated cells in comparison to controls, while the IκBα gene significantly decreased its expression in 1x and 2x IC_{50} of extract treatments compared to controls. In human HeLa cells treated with 0.5x IC_{50} of extract, the expression of the Bcl-2/Bax gene decreased by 0.5x compared to controls (Figure 4C). Nevertheless, under human HeLa cells treated with 1-IC_{50} of extract, the expressions of Bcl-2 , Bax , IL-6 , IL-8 , COX-2 , IKKα , NF-κB, IκBα, TNF-*a*, and IL-1β genes decreased by 0.034, 0.037, 0.119, 0.011, 0.048, 0.055, 0.065, 0.101, 0.561, and 0.083 times (Figure 4A, B, and D-K), respectively, compared with controls.

Discussion

The present study demonstrates that the extract possesses significant anti-cancer and antioxidant activities in HeLa cells. Treatment reduced cell viability, inhibited

Table II

Effects of *Gynura divaricata* on oxidative stress and antioxidant parameters

Parameter	Time (hour)	Control	DMSO (Vehicle control)	0.5x IC_{50}	1x IC_{50}	2x IC_{50}
H_2O_2 (µmole/µg protein)	0.5	2.2 ± 0.0	2.4 ± 0.0	3.8 ± 0.0[a]	2.5 ± 0.1[a]	2.0 ± 0.0[a]
	24	1.6 ± 0.1	1.7 ± 0.1	1.6 ± 0.0	2.7 ± 0.0[a]	2.6 ± 0.1[a]
MDA (µmole/mg protein)	0.5	14.2 ± 0.2	15.9 ± 0.4[a]	19.0 ± 0.3[a]	17.7 ± 0.4[a]	14.4 ± 0.3
	24	12.4 ± 0.1	13.8 ± 0.0[a]	11.2 ± 0.2*	12.4 ± 0.0	14.1 ± 0.3[a]
Ascorbate peroxidase (Unit/µg protein)	0.5	94.1 ± 33.2	83.9 ± 24.4	69.7 ± 23.1	73.3 ± 13.0	95.9 ± 24.0
	24	124.4 ± 26.7	133.6 ± 12.8	136.8 ± 21.9	140.1 ± 17.4	126.1 ± 36.1
Catalase (Unit/µg protein)	0.5	4.7 ± 0.2	6.1 ± 0.2	4.5 ± 0.3	4.3 ± 0.4	3.8 ± 0.2[a]
	24	11.9 ± 0.5	16.2 ± 1.2	6.4 ± 0.7[a]	4.7 ± 0.8[a]	3.7 ± 0.5[a]
Glutathione reductase (Unit/µg protein)	0.5	3.0 ± 0.1	3.4 ± 0.1	2.8 ± 0.2	2.4 ± 0.2[a]	2.6 ± 0.4
	24	6.7 ± 0.4	6.9 ± 0.5	6.0 ± 0.5	5.4 ± 0.3[a]	5.4 ± 0.2[a]
Superoxide dismutase (Unit/µg protein)	0.5	3.4 ± 0.5	4.5 ± 0.7	6.4 ± 0.4[a]	6.7 ± 0.7[a]	9.5 ± 1.2[a]
	24	7.8 ± 0.7	7.5 ± 0.8	8.1 ± 0.9	8.4 ± 0.7	12.3 ± 1.2[a]
DPPH scavenging (%)	0.5	6.2 ± 0.9	7.9 ± 1.1	10.1 ± 0.9[a]	10.1 ± 0.9[a]	9.8 ± 1.8[a]
	24	8.1± 0.5	6.1 ± 0.8	7.7 ± 0.8	6.1 ± 0.9	10.9 ± 0.7[a]
FRAP (µM Fe^{2+} equivalent)	0.5	24.8 ± 0.3	26.7 ± 0.3[a]	22.1 ± 0.4[a]	29.7 ± 0.7[a]	26.1 ± 0.4[a]
	24	24.9 ± 0.2	23.2 ± 0.2[a]	20.6± 0.2[a]	22.2 ± 0.3[a]	22.3 ± 0.2[a]

Values are mean ± SD; n=9; HeLa cell culture time period of 0.5 hour or 24 hours. Controls (without extract) were cells cultured in complete DMEM, while treatments were cells cultured in DMSO containing 500, 1,000, and 2,000 ng/mL of extract as 0.5x IC_{50}, 1x IC_{50}, and 2x IC_{50} concentrations; [a]p<0.05 is considered statistically significant in comparing controls and treatments of extract with HeLa cells across the same culture time period at 0.5 hour or 24 hours by Student's *t*-test

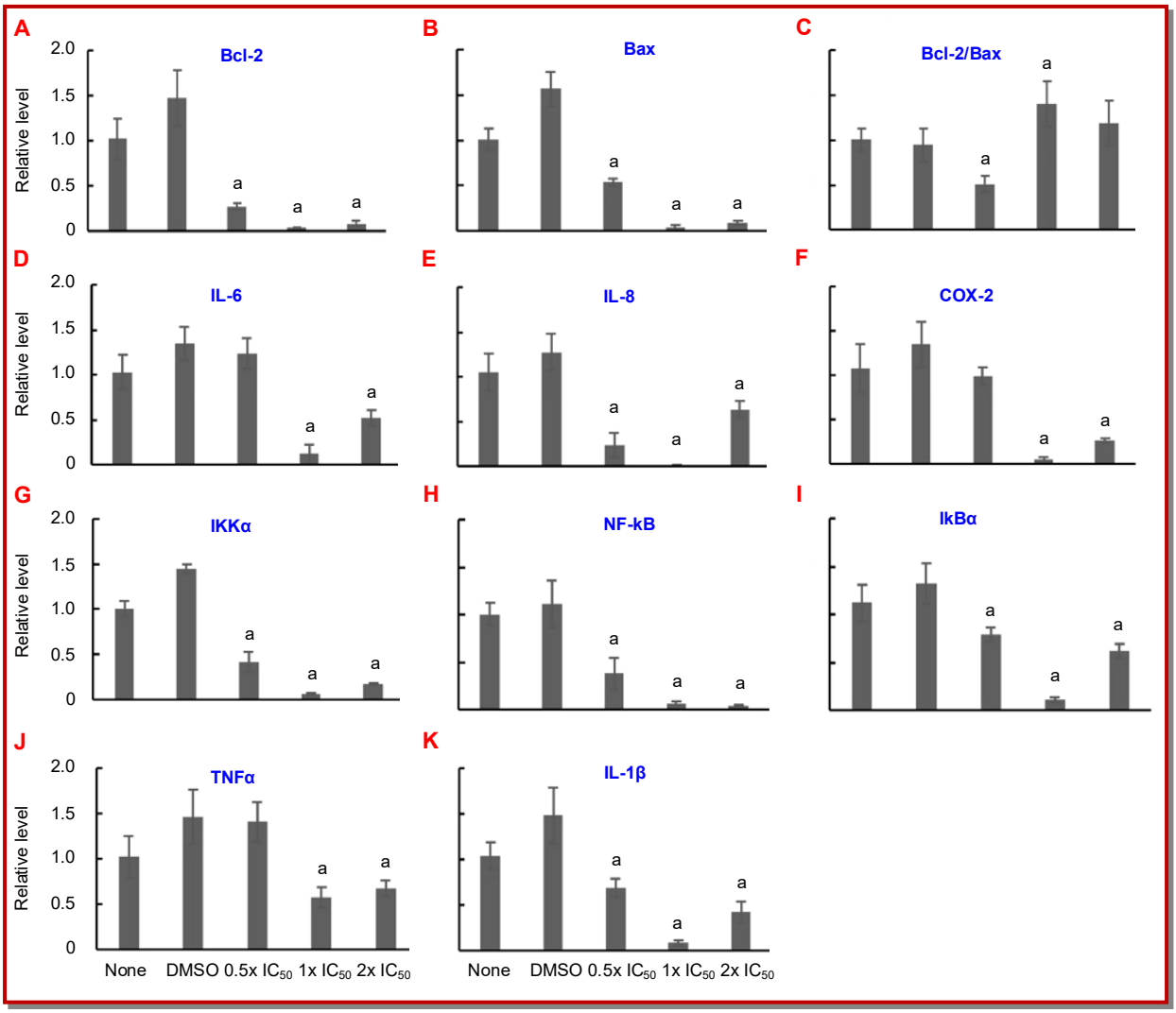

Figure 4: Relative RNA expressions of Bcl-2, Bax, Bcl-2/Bax ratio, IL-6, IL-8, COX-2, IKKα, NF-κB, IκBα, TNF-α, and IL-1β genes in control, DMSO, and extract-treated HeLa cells. Relative amounts were calculated using the $2^{-\Delta\Delta Ct}$ method and normalized with respect to GAPDH co-amplified as an internal control. Values are the means of three replicates with the corresponding standard deviation. The gene expression is compared to controls using Student's t-test, and superscript "a" indicates a significance level of $p \leq 0.05$. Controls were cells cultured in complete DMEM, while the treatments were cells cultured in DMSO containing 500, 1,000, and 2,000 ng/mL of extract as 0.5x IC_{50}, 1x IC_{50}, and 2x IC_{50} concentrations

cell migration, modulated oxidative stress biomarkers, enhanced antioxidant defense responses, and suppressed NF-κB signaling. The extract also regulated the expression of apoptosis- and inflammation-related genes, including Bcl-2, Bax, TNF-α, IL-6, IL-8, COX-2, IKKα, IκBα, and IL-1β. Collectively, these findings suggest that the extract may inhibit cervical cancer progression through coordinated regulation of oxidative stress, inflammatory signaling, and cell survival pathways.

The observed cytotoxic and anti-migratory effects are consistent with previous reports showing that plant-derived bioactive compounds suppress HeLa cell proliferation and migration (Rifai et al., 2024). Similar to earlier studies, the extract enhanced antioxidant defense mechanisms and reduced oxidative damage, supporting the role of antioxidant enzymes in protection against reactive oxygen species (Nguyen et al., 2018; Arora and Bhalata, 2017; Lin et al., 2020). The reduction of NF-κB signaling and inflammatory gene expression also agrees with reports indicating that inhibition of NF-κB is associated with decreased tumor growth, inflammation, and metastatic potential (Garcia-Pineres et al., 2009; Napetschnig and Wu, 2013; Li et al., 2016). Furthermore, the modulation of apoptosis-related genes is in accordance with studies showing that alterations in the Bcl-2/Bax regulatory network contribute to cancer cell death and growth suppression (Ryu et al., 2017; Yao et al., 2017; Maqbool et al., 2025). However, unlike some

studies that reported selective activation of pro-apoptotic signaling, the present study observed simultaneous regulation of both pro- and anti-apoptotic genes, suggesting a more complex mechanism of cellular adaptation and stress response.

The extract appears to influence intracellular redox balance by scavenging reactive oxygen species (ROS) and enhancing endogenous antioxidant defenses, thereby limiting lipid peroxidation and oxidative injury (Kumaran and Karunakaran, 2006; Dantu et al., 2012). Reduced oxidative stress may subsequently suppress NF-κB activation, leading to decreased expression of inflammatory mediators and adhesion-related molecules involved in cancer progression (Chao et al., 2013b; Cruceriu et al., 2020; Hayden and Ghosh, 2011). In addition, modulation of the Bcl-2/Bax signaling network may contribute to the regulation of apoptosis and cellular homeostasis (Gansukh et al., 2019; Kang et al., 2011; Chung and Yu, 2013). The coordinated down-regulation of NF-κB-associated genes may further impair cancer cell migration and metastatic behavior. These observations support the hypothesis that the extract exerts its anti-cancer effects through integrated regulation of oxidative stress, inflammation, apoptosis, and NF-κB-dependent signaling pathways. Nevertheless, the active constituents responsible for these effects remain unclear and require further investigation through mechanistic and *in vivo* studies.

Extract mitigates ROS accumulation and protects cellular components through the regulation of NF-κB–associated signaling, thereby suppressing cancer cell progression. Although extract demonstrates promising anti -cancer potential as a plant-derived therapeutic agent, its active constituents and precise molecular mechanisms within the NF-κB pathway remain unclear.

Limitation of this study includes *in vivo* studies that requires to elucidate its bioactivity, optimal dosage, and therapeutic efficacy as a safe natural antioxidant for clinical applications.

Conclusion

HeLa cell viability % significantly decreased upon expo -sure to increasing extract concentrations, showing that extract inhibited cell proliferation and increased the death rate of HeLa cells at high extract concentrations. Various extract dose-dependent manners also improved the antioxidant profiles of HeLa cells and exhibited relatively better DPPH radical scavenging activity and reducing power capacity to cope with oxidative stress.

Financial Support

Self-funded

Ethical Issue

The development, acquisition, authentication, cryopreservation, and transfer of cell lines between laboratories were followed according to the guidelines published in British Journal of Cancer, 2014

Conflict of Interest

Authors declare no conflict of interest

References

Arora D, Bhalata SC. Melatonin and nitric oxide regulate sunflower seedling growth under salt stress accompanying differential expression of Cu/Zn SOD and Mn SOD. Free Radic Biol Med. 2017; 106; 315-28.

Bradford MM. A rapid and sensitive method for the quantitation of microgram quantities of protein utilizing the principle of protein-dye binding. Anal Biochem. 1976; 72; 248-54.

Chao PY, Huang WY, Hu SP, Lo HF, Lin KK, Huang MY, Chang TR, Yang CM. Indigenous purple vegetable extracts protect against hydrogen peroxide -induced DNA damage in human lymphocytes. Food Nutr Sci. 2013a; 4; 62-70.

Chao PY, Huang WY, Hu SP, Lo HF. Lin KK, Huang MY, Chang TR, Yang CM. inhibitive effects of mulberry leaf-related extracts on cell adhesion and inflammatory response in human aortic endothelial cells. Evid Based Complement Alternat Med. 2013b; 1-14.

Chao PY, Liu YF, Lin KH, Lin SY, Hsu JI, Yang CM, Lai JY. Antioxidant activity in. extracts of 27 indigenous Taiwanese vegetables. Nutrients 2014; 6; 2115-30.

Chen CM, Li SC, Lin YL, Hsu CY, Shieh MJ, Liu JF. Consumption of purple sweet potato leaves modulates human immune response: T-lymphocyte functions, lytic activity of natural killer cell and antibody production. World J Gastroenterol. 2005; 11; 5777-81.

Chen J, Mangelinckx S, Ma L, Wang Z, Li W, Kimpe NDe. Caffeoylquinic acid derivatives isolated from the aerial parts of *Gynura divaricata* and their yeast alpha glucosidase and PTP1B inhibitory activity. Fitoterapia 2014; 99; 1-6.

Chou SC, Chuang LM, Lee SS. Hypoglycemic constituents of *Gynura divaricata* subsp. *Formosana*. Nat Prod Commun. 2012; 7; 221-22.

Chung KM, Yu SW. Interplay between autophagy and programmed cell death in mammalian neural stem cells. BMB Rep. 2013; 46; 383-90.

Cruceriu D, Baldasici O, Balacescu O, Berindan-Neagoe I. The dual role of tumor necrosis factor-alpha (TNF-α) in breast cancer: Molecular insights and therapeutic approaches. *Cell Oncol. 2020; 43*; 1-18.

Dantu AS, Shankarguru P, Devi DR. Evaluation of *in vitro* anticancer activity of hydroalcoholic extract of *Tabernaemontana divaricata*. Asian J Pharm Clin Res. 2012; 5; 59-61.

Dhindsa RA, Plumb-Dhindsa P, Thorpe TA. Leaf senescence:

Correlated with increased permeability and lipid peroxidation, and decreased levels superoxide dismutase and catalase. J Exp Bot. 1981; 126; 93-101.

Dong X, Zhao SX, Xu BQ, Zhang YQ. *Gynura divaricata* ameliorates hepatic insulin resistance by modulating insulin signalling, maintaining glycolipid homeostasis and reducing inflammation in type 2 diabetic mice. Toxicol Res. *2019;* 8; 928-38.

Feng X, Shan R, Xiaomeng H. The linkage of NF-κB signaling pathway-associated long non-coding RNAs with tumor microenvironment and prognosis in cervical cancer. BMC Med Genomics. 2023; 16; 169.

Foyer CH, Lopez-Delgado H, Dat JF, Scott IM. Hydrogen peroxide and glutathione associated mechanisms of acclamatory stress tolerance and signaling. Physiol Plant. 1997; 100; 241-54.

Gansukh E, Mya KK, Jung M, Keum YS, Kim DH, Saini RK. Lutein derived from marigold (*Tagetes erecta*) petals triggers ROS generation and activates Bax and caspase-3 mediated apoptosis of human cervical carcinoma (HeLa) cells. Food Chem Toxicol. 2019; 127; 11-18.

Garcia-Pineres AJ, Hildesheim A, Dodd L, Kemp TJ, Yang J, Fullmer B, Pinto LA. Gene expression patterns induced by HPV-16 L1 virus-like particles in leukocytes from vaccine recipients. J Immunol. 2009; 182; 1706-29.

Gugnoni M, Sancisi V, Manzotti G, Gandolfi G, Ciarrocchi A. Autophagy and epithelial–mesenchymal transition: An intricate interplay in cancer. Cell Death Dis. 2016; 7; e2520.

Hayden MS, Ghosh S.NF-κB in immunobiology. Cell Res. 2011; 21; 223-44.

He L, Xu X, Liu A, Sun J, Xue Y. Advances in studies on *Gynura divarica* (L.) DC. J Med Pharm Chin Minorities. 2014; 10; 61-65.

Hong MH, Jin X J, Yoon JJ, Lee YJ, Oh HC, Lee HS, Kim HY, Kang DG. Antihypertensive effects of *Gynura divaricata* (L.) DC in rats with renovascular hypertension. Nutrients 2020; 12; 3321.

Hou WC, Lin RD, Lee TH, Huang YH, Hsu FL, Lee MH. The phenolic constituents and free radical scavenging activities of *Gynura formosana* Kiamnra. J Sci Food Agri. 2005; 85; 615-21.

Jin X, Wang J, Xia Z, Miao X, Yin Y, Zhang Y. *Gynura divaricata* extract inhibits hepatocellular carcinoma growth via suppression of Wnt/β-catenin pathway. J Ethnopharmacol. 2018; 226; 141-49.

Kalsoom A, Altaf A, Sattar H, Maqbool T, Sajjad M, Jilani MJ, Shabbir G, Aftab S. Gene expression and anticancer evaluation of *Kigelia africana* (Lam.) Benth. extracts using MDA-MB -231 and MCF-7 cell lines. PloS one. 2024; 19; e0303134.

Kang H, Kwak Y, Koppula S. Protective effect of purple sweet potato (*Ipomoea batatas* Linn, Convolvulaceae) on neuroinflammatory responses in lipopolysaccharide-stimulated microglial cells. Trop J Pharm Res. 2014; 13; 1257-63.

Kang R, Zeh HJ, Lotze MT, Tang D. The beclin 1 network regulates autophagy and apoptosis. Cell Death Differ. 2011; 18; 571-80.

Kantawong F, Saisuwan C, Soeratanapant P, Wanachantararak P, Nan J, Wu J, Chang YT. *Gynura divaricata* water extract presented the possibility to enhance neuronal regeneration. Evid Based Complement Alternat Med. 2021; 8818618.

Kim HJ. Xu L, Chang KC, Shin SC, Chung J I, Kang D, Kim SH, Hur JA, Choi TH, Kim S, Choi J. Anti-inflammatory effects of anthocyanins from black soybean seed coat on the keratinocytes and ischemia-reperfusion injury in rat skin flaps. Microsurgery 2012; 32; 1-8.

Kosugi H, Kikugawa K. Thiobarbituric acid reaction of aldehydes and oxidized lipids in glacial acetic acid. Lipids 1985; 20; 915-20.

Kumaran A, Karunakaran RJ. Antioxidant and free radical scavenging activity of an aqueous extract of *Coleus aromaticus*. Food Chem. 2006; 97; 109-14.

Kumar P, Nagarajan A, Uchil PD. Analysis of cell viability by the MTT assay. Cold Spring Harb Protocol. 2018, p 6.

Lee SL, Chin TY, Tu SC, Wang YJ, Hsu YT, Kao MC, Wu YC. Purple sweet potato leaf extract induces apoptosis and reduces inflammatory adipokine expression in 3T3-L1 differentiated adipocytes. Evid Based Complement Alternat Med. 2015; 126302.

Li J, Feng J, Wei H. The aqueous extract of *Gynura divaricata* (L.) DC. improves glucose and lipid metabolism and amelio -rates type 2 diabetes mellitus. Evid Based Complement Alternat Med. 2018; 8686297.

Li J, Ma J, Wang KS, Mi C, Wang Z, Piao LX, Xu GH, Li X, Lee JJ, Jin X. Baicalein inhibits TNF-α-induced NF-κB activation and expression of NF-κB-regulated target gene products. Oncol Rep. 2016; 36; 2771-76.

Lin KH, Hsu CY, Huang YP, Lai JY, Hsieh WB, Huang MY, Yang CM, Chao PY. Chlorophyll-related compounds inhibit cell adhesion and inflammation in human aortic cells. J Med Food. 2013; 16; 886-98.

Lin KH, Lu CP, Chao JW, Yu YP. Antioxidant properties and anti-inflammatory effects of the hydroethanolic extracts of two varieties of bayberry fruit (*Myrica rubra* Sieb et Zucc.) prepared by stirring and ultrasonic methods. Not Bot Horti Agrobo. 2019; 47; 634-42.

Lin KH, Pan SF, Chen CC, Li WS, Chiang CM. Expression of human papillomavirus type 52 L1 capsid gene in *Oryza sativa* involved in cytoprotective activities. Not Bot Horti Agrobo. 2020; 48; 40-52.

Livak KJ, Schmittgen TD. Analysis of relative gene expression data using real-time quantitative PCR and the $2^{\Delta\Delta CT}$ method. Methods 2002; 25; 402-08.

Ma JF, Wei PF, Guo C, Shi YP, Lv Y, Qiu LX, Wen LP. The ethyl acetate extract of *Gynura formosana* Kitam. leaves inhibited cervical cancer cell proliferation via induction of autophagy. Biomed Res Int. 2018; 4780612.

Maqbool T, Faheem H, Sadia N, Inamullah I, Muhammad ABA, Muhammad R, Rabia R, Muhammad A, Awais A, Tahir M. Pulegone induced apoptotic and anti-proliferative potential in cervical cancer via P53, BAX and BCL2. Sci Rep. 2025; 15; 34217.

Morales M, Munne-Bosch S. Malondialdehyde: facts and

artifacts. Plant Physiol. 2019; 180; 1246-50.

Nadechanok J, Boonsom L, Saisunee L, John K, Stephen G. The chemical constituents and biological activities of the essential oil and the extracts from leaves of *Gynura divaricata* (L.) DC. growing in Thailand. J Essent Oil Bear Plant. 2015; 18; 543-55.

Nakano Y, Asada K. Hydrogen peroxide is scavenged by ascorbate-specific peroxidase in spinach chloroplasts. Plant Cell Physiol. 1981; 22; 867-80.

Napetschnig J, Wu H. Molecular basis of NF-κB signaling. Ann Rev Biophys. 2013; 42; 443-68.

Nguyen HC, Lin KH, Ho SL, Chiang CM, Yang CM. Enhancing the abiotic stress tolerance of plants: From chemical treatment to biotechnological approaches. Physiol Plant. 2018; 164; 452-66.

Oyaizu M. Antioxidative activities of browning products of glucosamine fractionated by organic solvent and thin layer chromatography. J Jpn Soc Nutr Food Sci. 1988; 35; 771-75.

Pasha A, Kumar K, Heena SK, Emerson IA. Pawar SC. Inhibition of NF-kB and COX-2 by andrographolide regulates the progression of cervical cancer by promoting PTEN expression and suppressing PI3K/AKT signalling pathway. Sci Rep. 2024; 14; 12020.

Rahman M, Asaeda T, Fukahori K, Imamura F, Nohara A, Matsubayashi M. Hydrogen peroxide measurement can be used to monitor plant oxidative stress rapidly using modified ferrous oxidation xylenol orange and titanium sulfate assay correlation. Int J Plant Biol. 2023; 14; 546-57.

Rifai FNP, Hidayah N, Sakinah FN, Adityani R. Cytotoxic and antiproliferative effects of *Gynura divaricata* ethanolic extract on HCT-116 colorectal cancer cells *in vitro*. Int. J. Cell Biomed. Sci. 2024; 3; 217-23.

Ryu R, Kim YJ, Kim KH. Antiproliferative activity of flavonoids from *Gynura divaricata* in breast cancer cell lines. Pharm Biol. 2017; 55; 2143-49.

Shen Z, Xu J, Wen L, Yin L, Cao X, Pei H, Zhao X. Bioassay-guide preparative separation of hypoglycemic components from *Gynura divaricata* (L.) DC by conventional and pH-zone refining countercurrent chromatography. Foods 2025; 4; 578.

Sun Y, Gao C. Liu H, Liu X, Yue T. Exploring the mechanism by which aqueous *Gynura divaricata* inhibits diabetic foot based on network pharmacology, molecular docking and experimental verification. Mol Med. 2023; 29; 11.

Wan C, Yu Y, Zhou S, Liu W, Tian S, Cao S. Antioxidant activity and free radical-scavenging capacity of *Gynura divaricata* leaf extracts at different temperatures. Pharmacogn Mag. 2011; 7; 40-45.

Xu B. Zhang Y. Bioactive components of *Gynura divaricata* and its potential use in health, food, and medicine: A mini-review. Afr J Tradit Complement Altern Med. 2017; 14; 113-27.

Xu C, Hu L, Zeng J, Wu A, Deng S, Zhao Z, Geng K. Luo J, Wang L, Zhou X, Huang W, Long Y, Song J, Zheng S, Wu J, Chen Q. *Gynura divaricata* (L.) DC. promotes diabetic wound healing by activating Nrf2 signaling in diabetic rats. J Ethnopharmacol. 2024; 323; 117638.

Xu W, Lu Z, Wang X, Cheung MH, Chen Y. *Gynura divaricata* exerts hypoglycemic effects by regulating the PI3K/AKT signaling pathway and fatty acid metabolism signaling pathway. Nutr Diabetes. 2020; 10; 31.

Yao C, Cao X, Fu Z, Tian J, Dong W, Xu J, An K, Zhai L, Yu J. *Boschniakia rossica* polysaccharide triggers laryngeal carcinoma cell apoptosis by regulating expression of Bcl-2, caspase-3, and p53. Med Sci Monit. 2017; 23; 2059-64.

Ye X, Wang L, Yang X, Yang J, Zhou J, Lan C, Kantawong F, Kumsaiyai W, Wu J, Zeng J. Integrated chemical characterization, network pharmacology and transcriptomics to explore the mechanism of sesquiterpenoids isolated from *Gynura divaricata* (L.) DC. against chronic myelogenous leukemia. Pharmaceuticals 2022; 15; 1435.

Yen CH, Lai CC, Shi TH, Chen M, Yu HC, Liu YP, Chang FR. *Gynura divaricata* attenuates tumor growth and tumor relapse after cisplatin therapy in HCC xenograft model through suppression of cancer stem cell growth and Wnt/β-catenin signalling. J Ethnopharmacol. 2018; 213; 366-75.

Yoon SS, Moon EY. B-cell adhesion to fibroblast-like synoviocytes is up-regulated by tumor necrosis factor-alpha via expression of human vascular cell adhesion molecule-1 mediated by beta cell-activating factor. Int J Mol Sci. 2021; 22; 7166.

Author Info

Chih-Ming Chiang (Principal contact)
e-mail: cmchiang@mail.mcu.edu.tw